On the connection between the self-sputter yield and deposition rate in HiPIMS operation

J. T. Guðmundsson[1,2], M. Rudolph[3], K. Barynova[1], J. Fischer[4], S. Suresh Babu[1], N. Brenning[2,4], M. A. Raadu[2], H. Hajihoseini[5] and D. Lundin[4]

[1] Science Institute, University of Iceland, Reykjavik, Iceland
[2] KTH Royal Institute of Technology, Stockholm, Sweden
[3] Leibniz Institute of Surface Engineering (IOM), Leipzig, Germany
[4] Plasma and Coatings Physics, Linköping University, Sweden
[5] Industrial Focus Group XUV Optics, University of Twente, The Netherlands

The 49th International Conference on Metallurgical Coatings and Thin Films (ICMCTF), San Diego, California, May 25., 2023

Introduction – Magnetron sputtering

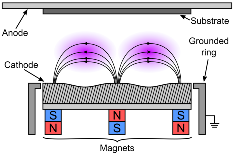

Gudmundsson and Lundin (2020) in High Power Impulse Magnetron Sputtering Discharge, Elsevier, 2020

- Magnetron sputtering has been a highly sucessfull technique that is essential in a number of industrial applications Gudmundsson (2020) PSST **29** 113001
- In a high power impulse magnetron sputtering (HiPIMS) the discharge is driven by high power pulses of low repetition frequency, and with low duty cycle
- This results in high discharge current density, increased electron density, and increased ionization of the sputtered species Gudmundsson et al. (2012) JVSTA **30** 030801

Overview

- Thin film deposition
- The ionization region model (IRM)
- Deposition rate vs ionized flux fraction
- Working gas rarefaction
- Summary

Thin film deposition

Thin film deposition

- The film mass density is always higher when depositing with HiPIMS compared to dcMS at the same average power
- The surfaces are significantly smoother when depositing with HiPIMS compared to dcMS
- The films typically exhibit better crystallinity, and overall improved film properties
    - lower electrical resistivity
    - improved optical properties
    - improved mechanical properties
    - better oxidation resistance

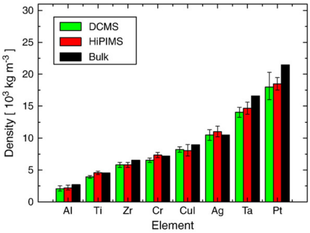

From Samuelsson et al. (2010) SCT **202** 591

Thin film deposition

- TiN as diffusion barriers for copper and aluminum interconnects
- HiPIMS deposited films have significantly lower resistivity than dcMS deposited films on SiO_2 at all growth temperatures
- Thus, ultrathin continuous TiN films with superior electrical characteristics and high resistance towards oxidation can be obtained with HiPIMS at reduced temperatures compared to dcMS

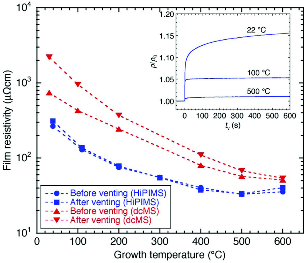

From Magnus et al. (2012) IEEE EDL **33** 1045

Thin film deposition

- There is a drawback
- The deposition rate is lower for HiPIMS when compared to dcMS operated at the same average power
- The HiPIMS deposition rates are typically in the range of 30 – 85% of the dcMS rates depending on target material
- Many of the ions of the target material are attracted back to the target surface by the cathode potential

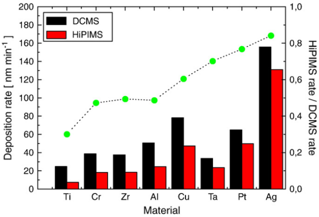

From Samuelsson et al. (2010) SCT **202** 591

The ionization region model (IRM)

Ionization region model

- The ionization region model (IRM) is a time-dependent volume averaged plasma chemical model of the ionization region (IR) of the HiPIMS discharge
- The IRM gives the temporal evolution of the densities of ions, neutrals and electrons
- The IRM gives also two internal parameters that are of importance
  - α_t – ionization probability
  - β_t – back-attraction probability

Detailed model description is given in Huo et al. (2017) JPD **50** 354003

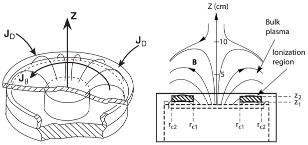

The definition of the volume covered by the IRM

- The IR is defined as an annular cylinder of width $w_{rt} = r_{c2} - r_{c1}$ and thickness $L = z_2 - z_1$, extends from z_1 to z_2 axially away from the target

From Raadu et al. (2011) PSST **20** 065007

Ionization region model

- The temporal development is defined by a set of ordinary differential equations giving the first time derivatives of
  - the electron energy
  - the particle densities for all the particles (except electrons)
- The species assumed in the non-reactive-IRM are
  - cold electrons e^{C}, hot electrons e^{H}
  - argon atoms $Ar(3s^2 3p^6)$, warm argon atoms in the ground state Ar^{W}, hot argon atoms in the ground state Ar^{H}, Ar^{m} ($1s_5$ and $1s_3$) (11.6 eV), argon ions Ar^{+} (15.76 eV), doubly ionized argon ions Ar^{2+} (27.63 eV)
  - Metal atoms, sometimes metastable states, metal ion M^{+}, and doubly ionized metal ions M^{2+}

Detailed model description is given in Huo et al. (2017), JPD **50** 354003

Ionization region model

- As an example the particle balance equation for the metal ion M^+ is

$$\frac{\mathrm{d}n_{\mathrm{M^+}}}{\mathrm{d}t} = \underbrace{k_{\mathrm{iz,M}}^{\mathrm{c}} n_{\mathrm{e}} n_{\mathrm{M}} + k_{\mathrm{iz,M}}^{\mathrm{h}} n_{\mathrm{e}} n_{\mathrm{M}}}_{\text{electron impact ionization}} + \underbrace{k_{\mathrm{P,iz}} n_{\mathrm{Ar^m}} n_{\mathrm{M}}}_{\text{Penning ionization}}$$

$$+ \underbrace{k_{\mathrm{chexc,1}} n_{\mathrm{M}} n_{\mathrm{Ar^+}} + k_{\mathrm{chexc,2}} n_{\mathrm{M^{2+}}} n_{\mathrm{Ar}}}_{\text{charge exchange}} - \underbrace{k_{\mathrm{iz,M^+}}^{\mathrm{c}} n_{\mathrm{e}} n_{\mathrm{M^+}} - k_{\mathrm{iz,M^+}}^{\mathrm{h}} n_{\mathrm{e}} n_{\mathrm{M^+}}}_{\text{electron impact ionization to create } \mathrm{M^{2+}}}$$

$$- \underbrace{\frac{\Gamma_{\mathrm{M^+}}^{\mathrm{RT}} + \Gamma_{\mathrm{M^+}}^{\mathrm{BP}} (S_{\mathrm{IR}} - S_{\mathrm{RT}})}{V_{\mathrm{IR}}}}_{\text{ion flux out of the ionization region}}$$

Ionization region model

- The IRM is a semi-empirical discharge model and requires the measured discharge current and voltage waveforms
- The IRM has three unknown fitting parameters
  - the ion back-attraction probability for the metal ions $\beta_{\mathrm{t,pulse}}$ and gas ions $\beta_{\mathrm{g,pulse}}$
  - the potential drop across the IR $f = V_{\mathrm{IR}}/V_{\mathrm{D}}$
  - the electron recapture probability $r = 0.7$
- This leaves the ($\beta_{\mathrm{t,pulse}}$, f) parameter space to be explored through the model fitting procedure – the blue zones in the fitting map indicate the smallest mean square error

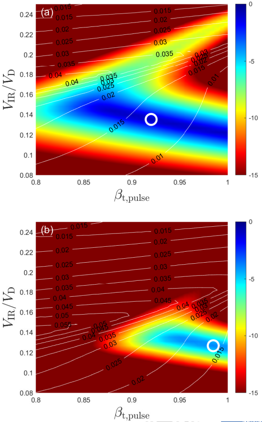

Graphite target from Eliasson et al. (2021) PSST **29** 115017

Ionization region model

- The ionization probability α_t increases with increased discharge voltage
- The peak discharge current increases with increased discharge voltage
- Earlier we have argued that the ionization probability depends only on the peak discharge current and increases with increased peak discharge current

Rudolph et al. (2022) JPD **55** 015202

- The back-attraction probability $\beta_{t,pulse}$ decreases with increased discharge voltage

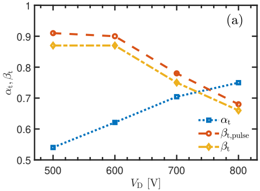

A discharge with tungsten target

From Suresh Babu et al. (2022) PSST **31** 065009

Ionization region model

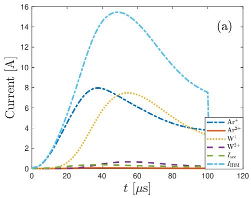

W: PSST (2022) **31** 065009

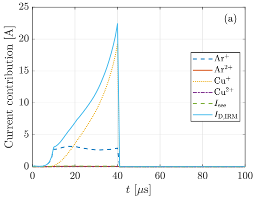

Cu: SCT (2022) **442** 128189

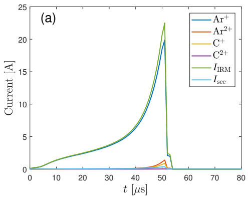

C: PSST (2021) **30** 115017

- The temporal evolution of the discharge current composition at the target surface for three different targets
- With Cu target Cu^+ ions dominate, with graphite target Ar^+ ions dominate

Deposition rate vs ionized flux fraction

Deposition rate – α_t and β_t

- We can relate the measured quantities normalized deposition rate $F_{\mathrm{DR,sput}}$ and the ionized flux fraction $F_{\mathrm{ti,flux}}$

$$F_{\mathrm{DR,sput}} = \frac{\Gamma_{\mathrm{DR}}}{\Gamma_0} = (1 - \alpha_t \beta_t)$$

$$F_{\mathrm{ti,flux}} = \frac{\Gamma_{\mathrm{DR,ions}}}{\Gamma_{\mathrm{DR,sput}}} = \frac{\Gamma_0 \alpha_t (1 - \beta_t)}{\Gamma_0 (1 - \alpha_t \beta_t)} = \frac{\alpha_t (1 - \beta_t)}{(1 - \alpha_t \beta_t)}$$

to the internal parameters back attraction probability β_t

$$\beta_t = \frac{1 - F_{\mathrm{DR,sput}}}{1 - F_{\mathrm{DR,sput}}(1 - F_{\mathrm{ti,flux}})}$$

and ionization probability α_t

$$\alpha_t = 1 - F_{\mathrm{DR,sput}}(1 - F_{\mathrm{ti,flux}})$$

Hajihoseini et al. (2019) *Plasma* **2** 201 and later refined by Rudolph et al. (2021) JAP **129** 033303

Deposition rate – Optimization

- There are two measures of how good a HiPIMS discharge is:
  - the fraction $F_{\mathrm{DR,sput}}$ of all the sputtered material that reaches the diffusion region (DR)
  - the fraction $F_{\mathrm{ti,flux}}$ of ionized species in that flux
- There is a trade off between the goals of higher $F_{\mathrm{DR,sput}}$ and higher $F_{\mathrm{ti,flux}}$
- The question that remains:
  - How can we vary the ionization probability α_{t} and maybe more importantly the back-attraction probability β_{t} ?

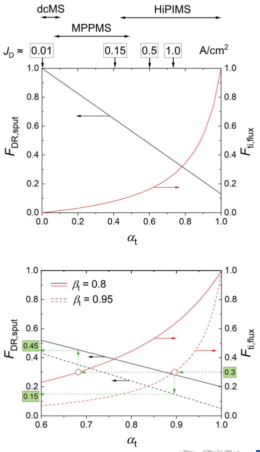

From Brenning et al. (2020) *JVSTA* **38** 033008

Deposition rate – Optimization

- What determines the back-attraction probability ?
- How can one influence the back-attraction probability ?
- The back-attraction probability $\beta_{\rm t,pulse}$, determined by IRM, versus the self-sputter yield for various target materials
- The data indicate that the back-attraction probability decreases roughly linearly with increased self-sputter yield

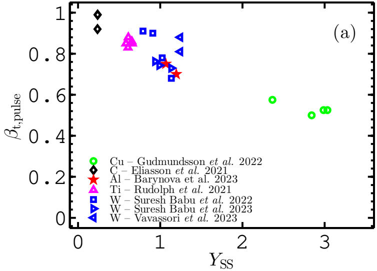

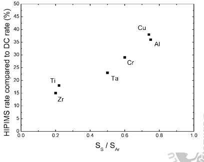

Helmersson et al. (2005) SVC Conf. Proc. 2005, p. 458

Working gas rarefaction

Working gas rarefaction

- The sputtered species enter the discharge at considerable energy, which is determined by the cohesive energy of the solid target
- The interaction between the energetic sputtered particles and the working gas atoms can lead to a reduction in the working gas density – as has been observed experimentally in the HiPIMS discharge
- The maximum in the degree of working gas rarefaction, determined by the IRM, for various target materials versus the peak discharge current density $J_{D,peak}$

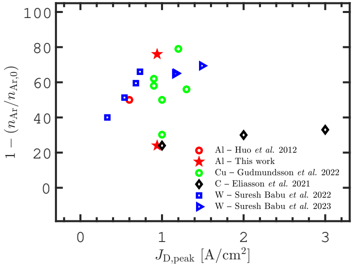

From Barynova et al. to be submitted

Working gas rarefaction

- HiPIMS discharge with graphite target and $J_{\mathrm{D,peak}} = 1$ A cm^{-2}

  Eliasson et al. (2021) PSST **30** 115017

- Argon atoms are lost mainly through electron impact ionization by primary and secondary electrons
- Contributions of kick-out and charge-exchange are negligible
- Diffusion contributes to a net loss of argon atoms during the pulse, but to a flow into the ionization region after the pulse is off

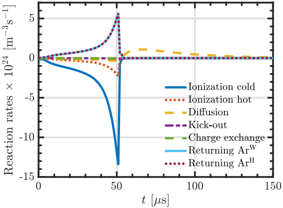

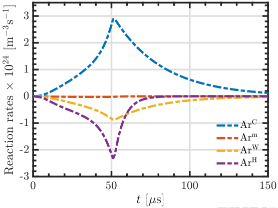

From Barynova et al. to be submitted

Working gas rarefaction

- HiPIMS discharge with tungsten target and $J_{\mathrm{D,peak}} = 0.54$ A cm^{-3}

  Suresh Babu et al. (2022) PSST **31** 065009

- The main contributor to the loss of argon atoms from the IR is kick-out by tungsten atoms sputtered from the target (39 – 48 % contribution)
- The second most important loss process is electron impact ionization by secondary electrons followed by electron impact ionization by the primary electrons

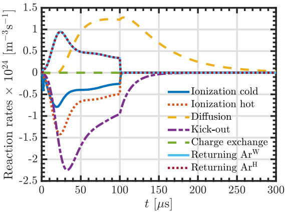

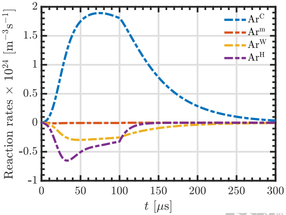

From Barynova et al. to be submitted

Working gas rarefaction

- The relative contributions of the various processes to working gas rarefaction varies greatly depending on the target material
- The various contributions versus the atomic mass of the target material for $J_{\mathrm{D,peak}} \sim 1$ A/cm^2 and $p_{\mathrm{g}} \sim 1$ Pa
- Electron impact ionization by primary electrons is rather significant for a graphite target, but its role decreases with increased atomic mass
- The role of kick-out, or the sputter wind, increases with increased mass of the target atom

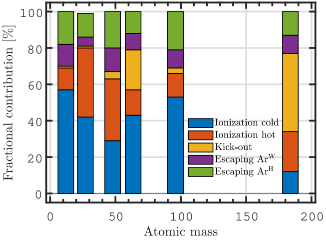

From Barynova et al. to be submitted

Summary

Summary

- The discharge current composition at the target surface depends on the target material
- There is an inescapable conflict between the goals of higher deposition rate and higher fraction of ionized species in the sputtered material flux
- The back-attraction probability appears to depend on the self-sputter yield – it is lower for higher self-sputter yield
- The main contributor to working gas rarefaction for low mass target atoms is electron impact ionization, while for heavy mass target atoms kick-out by the sputtered species is the main contributor

Thank you for your attention

tumi@hi.is

The slides can be downloaded at

http://langmuir.raunvis.hi.is/~tumi/ranns.html

Further reading

- J. T. Gudmundsson, Physics and technology of magnetron sputtering discharges, Plasma Sources Science and Technology, **29**(11) (2020) 113001
- J. T. Gudmundsson, André Anders, and Achim von Keudell, Foundations of physical vapor deposition with plasma assistance, Plasma Sources Science and Technology, **31**(8) (2022) 083001
- Daniel Lundin, Tiberiu Minea and Jon Tomas Gudmundsson (eds.), High Power Impulse Magnetron Sputtering: Fundamentals, Technologies, Challenges and Applications, Elsevier, 2020


Topical Review

Physics and technology of magnetron sputtering discharges

J T Gudmundsson


Topical Review

Foundations of physical vapor deposition with plasma assistance

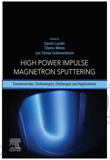

References

Brenning, N., A. Butler, H. Hajihoseini, M. Rudolph, M. A. Raadu, J. T. Gudmundsson, T. Minea, and D. Lundin (2020). Optimization of HiPIMS discharges: The selection of pulse power, pulse length, gas pressure, and magnetic field strength. *Journal of Vacuum Science and Technology A 38*(3), 033008.

Eliasson, H., M. Rudolph, N. Brenning, H. Hajihoseini, M. Zanáška, M. J. Adriaans, M. A. Raadu, T. M. Minea, J. T. Gudmundsson, and D. Lundin (2021). Modeling of high power impulse magnetron sputtering discharges with graphite target. *Plasma Sources Science and Technology 30*(11), 115017.

Gudmundsson, J. T. (2020). Physics and technology of magnetron sputtering discharges. *Plasma Sources Science and Technology 29*(11), 113001.

Gudmundsson, J. T., N. Brenning, D. Lundin, and U. Helmersson (2012). The high power impulse magnetron sputtering discharge. *Journal of Vacuum Science and Technology A 30*(3), 030801.

Gudmundsson, J. T. and D. Lundin (2020). Introduction to magnetron sputtering. In D. Lundin, T. Minea, and J. T. Gudmundsson (Eds.), *High Power Impulse Magnetron Sputtering: Fundamentals, Technologies, Challenges and Applications*, pp. 1–48. Amsterdam, The Netherlands: Elsevier.

Hajihoseini, H., M. Čada, Z. Hubička, S. Ünaldi, M. A. Raadu, N. Brenning, J. T. Gudmundsson, and D. Lundin (2019). The effect of magnetic field strength and geometry on the deposition rate and ionized flux fraction in the HiPIMS discharge. *Plasma 2*(2), 201–221.

Helmersson, U., M. Lattemann, J. Alami, J. Bohlmark, A. P. Ehiasarian, and J. T. Gudmundsson (2005). High power impulse magnetron sputtering discharges and thin film growth: A brief review. In *Proceedings of the 48th Society of Vacuum Coaters Annual Technical Conferenece*, pp. 458 – 464.

Huo, C., D. Lundin, J. T. Gudmundsson, M. A. Raadu, J. W. Bradley, and N. Brenning (2017). Particle-balance models for pulsed sputtering magnetrons. *Journal of Physics D: Applied Physics 50*(35), 354003.

References

Magnus, F., A. S. Ingason, S. Olafsson, and J. T. Gudmundsson (2012). Nucleation and resistivity of ultrathin TiN films grown by high power impulse magnetron sputtering. *IEEE Electron Device Letters 33*(7), 1045 – 1047.

Raadu, M. A., I. Axnäs, J. T. Gudmundsson, C. Huo, and N. Brenning (2011). An ionization region model for high power impulse magnetron sputtering discharges. *Plasma Sources Science and Technology 20*(6), 065007.

Rudolph, M., N. Brenning, H. Hajihoseini, M. A. Raadu, T. M. Minea, A. Anders, D. Lundin, and J. T. Gudmundsson (2022). Influence of the magnetic field on the discharge physics of a high power impulse magnetron sputtering discharge. *Journal of Physics D: Applied Physics 55*(1), 015202.

Rudolph, M., H. Hajihoseini, M. A. Raadu, J. T. Gudmundsson, N. Brenning, T. M. Minea, A. Anders, and D. Lundin (2021). On how to measure the probabilities of target atom ionization and target ion back-attraction in high-power impulse magnetron sputtering. *Journal of Applied Physics 129*(3), 033303.

Samuelsson, M., D. Lundin, J. Jensen, M. A. Raadu, J. T. Gudmundsson, and U. Helmersson (2010). On the film density using high power impulse magnetron sputtering. *Surface and Coatings Technology 202*(2), 591–596.

Suresh Babu, S., M. Rudolph, D. Lundin, T. Shimizu, J. Fischer, M. A. Raadu, N. Brenning, and J. T. Gudmundsson (2022). Ionization region model of a high power impulse magnetron sputtering of tungsten. *Plasma Sources Science and Technology 31*(6), 065009.